Journal of Colloid and Interface Science 485 (2017) 59–64

Contents lists available at ScienceDirect

Journal of Colloid and Interface Science

journal homepage: www.elsevier.com/locate/jcis

Regular Article

Sorption and redox speciation of plutonium at the illite surface under highly saline conditions

Rémi Marsac [a,b], Nidhu lal Banik [a,c], Johannes Lützenkirchen [a,*], Alexandre Diascorn [a,d], Kerstin Bender [a], Christian Michael Marquardt [a], Horst Geckeis [a]

[a] Institut für Nukleare Entsorgung, Karlsruhe Institute of Technology, P.O. Box 3640, D-76021 Karlsruhe, Germany
[b] Ecole Nationale Supérieure de Chimie de Rennes, UMR CNRS 6226, 11 Allée de Beaulieu, F-35708 Rennes Cedex 7, France[1]
[c] Institute for Transuranium Elements, European Commission, P.O. Box 2340, D-76125 Karlsruhe, Germany[1]
[d] Groupe d'Etudes Atomiques (GEA), Ecole des Applications Militaires de l'Energie Atomique (EAMEA). BCRM Cherbourg, CC19 50115 Cherbourg-Octeville Cedex, France[1]

GRAPHICAL ABSTRACT

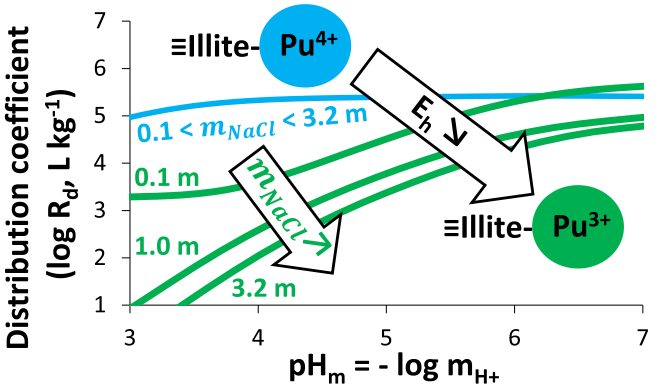

ARTICLE INFO

Article history:
Received 27 June 2016
Revised 19 August 2016
Accepted 8 September 2016
Available online 13 September 2016

Keywords:
Plutonium
Illite
Clay
Saline
Speciation
Redox
Sorption
Surface complexation model
Ion exchange

ABSTRACT

Natural groundwater may contain high salt concentrations, such as those occurring at several potential deep geological nuclear waste repository sites. Actinide sorption to clays (e.g. illite) under saline conditions has, however, been rarely studied. Furthermore, both illite surface and ionic strength may affect redox speciation of actinides like plutonium. In the present study, Pu sorption to illite is investigated under anaerobic conditions for $3 < pH_m$ (=−log m_{H^+}) < 10 and m_{NaCl} = 1.0 and 3.2 molal (m). Results are compared with previous data for m_{NaCl} = 0.1 m. According to redox potential measurements and based on Eu(III)-illite sorption data (taken as analogue of Pu(III)), the strong effect of m_{NaCl} on overall Pu uptake observed for $pH_m < 6$ is mainly attributed to the presence of Pu(III) and its competition with Na^+ for ion exchange sites. For $pH_m > 6$, overall Pu uptake is largely insensitive to m_{NaCl} due to the prevalence of strongly adsorbed Pu(IV). By applying appropriate corrections to the activity coefficients of dissolved ions and using the 2-site protolysis non-electrostatic surface complexation and cation exchange (2 SPNE SC/CE) model, experimental data on Pu sorption to illite as a function of pH, Eh and m_{NaCl} can be very well reproduced.

* Corresponding author.
E-mail address: johannes.luetzenkirchen@kit.edu (J. Lützenkirchen).
[1] Present address.

http://dx.doi.org/10.1016/j.jcis.2016.09.013
0021-9797/

1. Introduction

Only few investigations of actinide uptake on clay minerals have been carried out at elevated ionic strength (I) [1–3]. The majority of investigations pertains to I = 0.1 molal (m) and rarely up to 1.0 m (e.g. [4–6]; and references therein). However, clay rock pore waters as e.g. in the Jurassic and lower Cretaceous clay rock in Northern Germany, discussed as potentially appropriate host rock formations for a final nuclear waste repository, may contain salt contents as high as about 5 m [7]. Sedimentary rocks currently investigated in Canada are in contact with brine solutions up to 6.5 m [8]. Therefore, detailed sorption investigations of radionuclide onto clay materials under saline conditions become necessary. At high salt concentrations, activity coefficients of aqueous species change dramatically and actinide cations may form aqueous complexes with background anions, which can affect actinide speciation (including redox equilibria). But this can in principle be predicted. By contrast, the effect of high ionic strength on mineral (i.e. including clay minerals) surface properties is elusive. Previous studies performed at high ionic strength show that non-electrostatic sorption models are quite suitable to simulate proton and metal ion sorption to naturally occurring surfaces, e.g. marine microalgae or bacteria [9–11]. Recently, Eu(III) sorption to illite and smectite was investigated in 0.1 < m_{NaCl} < 3.9 m [3]. The experimental results could be described by the 2 site protolysis non-electrostatic surface complexation and cation exchange (2 SPNE SC/CE) model [5,6] coupled to the specific ion interaction theory (SIT [12]) or the Pitzer formalism [13], to account for activity coefficients of solutes in concentrated media.

Compared to Eu(III), the complex redox chemistry of Pu adds another dimension to sorption studies. Pu occurs in the oxidation states +III, +IV, +V or +VI and its geochemical behavior, such as solubility and mobility, strongly depends on its redox state [14,15]. Under reducing conditions, Pu(IV) and Pu(III) prevail [16–20]. However, Pu(III) sorption to minerals has rarely been studied separately as it is usually accompanied by Pu(IV). It has been shown, that the overall uptake of redox sensitive actinides and their redox speciation at mineral surfaces can be estimated by taking into account the uptake of the individual redox states and the measured redox potentials, i.e. the (apparent) electron activity, or pe [21,22]. Using the 2 SPNE SC/CE model, previous work demonstrated the applicability of the approach to describe Pu uptake on illite under anaerobic conditions in 0.1 m NaCl, where the Pu(IV)/Pu(III) redox couple was involved [23]. Here, the approach is extended to Pu sorption and redox speciation in contact with illite under saline conditions (up to 3.2 m NaCl). While there is no study dedicated to tetravalent actinide sorption to illite at such high ionic strength, Eu(III) sorption to illite (often studied as chemical analogue of Pu (III)) is affected by NaCl concentration [3]. Therefore, Pu sorption and Pu(IV)/Pu(III) redox equilibria at the illite surface are expected to be affected by the ionic strength.

2. Materials and methods

Chemicals (all pro analytical quality or better) were obtained from Merck (Darmstadt, Germany) or Riedel de Haen (Seelze, Germany). Solutions were prepared with de-ionized "MilliQ" water (specific resistivity, 18.2 MΩ cm^{-1}). The purified Na-illite was provided within the EC project CP CatClay. The source material derives from lacustrine continental sediments deposited at the Upper Eocene (~−35 Ma) in the basin of Le Puy en Velay (Massif Central, France). The purification procedures and the characterization of the purified illite (<63 μm) were previously detailed [21], and will not be repeated here. Note that in the last step of the purification, the clay suspension was freeze dried, to exclude bacterial activity.

2.1. Plutonium and Europium stock solutions

A ^{238}Pu stock solution was prepared from an available Pu solution dissolved in nitric acid, which was fumed three times by 0.1 M $HClO_4$, in order to remove all impurities and organic traces. The concentration of the Pu stock solution was 3.9×10^{-5} M in 0.1 M $HClO_4$. From this, a more dilute solution ([Pu] = 1.9×10^{-6} M) in 0.1 M $HClO_4$ was prepared for experiments at low Pu(IV) concentration. The diluted ^{238}Pu stock solution contained 85% Pu(IV), 11% Pu(V) and 4% Pu(III), as determined by liquid-extraction methods [23]. Aqueous ^{238}Pu concentrations were determined by liquid scintillation counting (LSC) using the scintillation cocktail Ultima Gold XR with a liquid scintillation analyzer (Tri-Carb 3110TR). In addition, the stock solution of ^{238}Pu was checked by ICP-MS and the results were in excellent agreement with LSC measurements.

Eu(III) was used in some experiments as a chemical analogue of Pu(III). A radiotracer solution was purchased from Amersham International (total Eu concentration: 6.0×10^{-4} M) with isotopic composition ^{151}Eu (83%), ^{152}Eu (13%, $t_{1/2}$ = 13.33a) and ^{153}Eu (4%). ^{152}Eu is a β-, γ-emitter and can be conveniently analyzed by γ-counting. In the present study, precise determination of dissolved ^{152}Eu was performed using a Perkin Elmer Wallac gamma counter (Wizard 1480).

2.2. Determination of pH and Eh

The pH in the clay suspensions was measured by an Orion 525A (pH meter) and a Ross electrode calibrated with 4 standard buffers (pH 3, 5, 7, and 9; Merck). The error in pH measurements is ±0.05. For pH measurements in highly saline conditions (I > 0.1 m) a correction term is applied to the measured operational pH-values (pH_{exp}). The molal proton concentration, i.e. $-\log m_{H^+}$ (pH_m), was obtained involving an empirical correction coefficient (A_{NaCl}) according to Eqs. (1) and (2):

$$pH_m = pH_{exp} + A_{NaCl} \quad (1)$$

$$A_{NaCl} = 0.0013 * (m_{NaCl})^2 + 0.1715 * m_{NaCl} - 0.0988 \quad (2)$$

A_{NaCl} depends on background electrolyte composition and concentration and has been accurately determined for NaCl solutions for the electrodes we use [24]. m_{NaCl} is the molality (mol kg^{-1}) of the background electrolyte.

The redox potentials in the clay suspensions were measured using an Orion 525A (E_h meter) and a Pt electrode combined with a Ag/AgCl reference system (Metrohm). Raw data were converted into Eh vs. standard hydrogen electrode (SHE) by correcting for the potential of the reference electrode. Eh was converted to the negative logarithm of the apparent electron activity, pe = $-\log a_{e^-}$ = 16.9 × Eh(V) at 25 °C. A commercial redox-buffer (220 mV, Schott instruments) was used for calibration. An equilibration time of 15 min was allowed for all Eh measurements, after having stirred the suspension. Uncertainties in Eh measurements are ±50 mV (±0.8 for pe-scale) [20,25]. Unlike for the measurement of pH, to our knowledge, there is no ionic strength dependent correction to apply to the experimental Eh with the presently used set-up.

2.3. Batch sorption experiments

All sorption studies were performed as batch type experiments. The procedure is the same as in our previous work dedicated to m_{NaCl} = 0.1 m [23]. The effect of pH_m was investigated at an initial Pu concentration ($[Pu]_{tot}$) of 8×10^{-11} M in 3.2 m NaCl. In addition, the effect of $[Pu]_{tot}$ was investigated for m_{NaCl} = 1.0 and 3.2 m, $8 \times 10^{-11} < [Pu]_{tot} < 10^{-8}$ M and $pH_m \approx 4.5$, 6 and 9.5. Batch experiments were carried out in 40 mL polypropylene centrifuge tubes at room temperature in an argon glove box (<1 ppm O_2, absence

of CO_2). The suspension volume was 25 mL. At a solid to liquid ratio of 2 g L^{-1}, the suspensions were preconditioned in 1 or 3.2 m NaCl under continuous shaking for 4–5 days to achieve a given target pH_m value by adding 0.1 M HCl or 0.1 M NaOH. After adding Pu to the illite suspension, pH_m was adjusted again to the respective target pH_m. Neither pH nor Eh buffers were used. The vials were then closed and shaken end-over-end. According to previous studies [23,26–29], potentially occurring redox processes might be rather slow. Consequently, an equilibration time of one year was chosen to make sure that equilibrium was established [23,28]. After one year, pH_{exp} and Eh were measured in the suspension and an aliquot of each sample was transferred to a centrifuge tube (Beckmann, Recorder No.: 356562) and centrifuged (Beckmann Coulter XL-90 K) at 90,000 rpm (~700,000*g* max) for one hour. The supernatant was analyzed for dissolved Pu by LSC.

Results from the batch experiments will be expressed throughout as distribution coefficients (R_d in L kg^{-1}), calculated by the following equation:

$$R_d = ([Pu]_{tot}/[Pu]_{aq} - 1) \times V/m \quad (3)$$

where $[Pu]_{aq}$ and $[Pu]_{tot}$ (M) are the dissolved (final) equilibrium and total (initial) concentrations of Pu, respectively. The term V/m corresponds to the aqueous solution volume to illite mass ratio (L kg^{-1}). According to a previous experimental study [23], an uncertainty of ±0.2 is assigned to log R_d, although it could be larger according to comparable studies where >99% uptake is obtained [6]. Under such conditions, larger uncertainties are induced by analytical constraints.

Batch Eu sorption experiments were performed for $[Eu]_{tot} = 3 - \times 10^{-9}$ M applying the same protocol as for Pu, except that Eh was not recorded because Eu is not redox sensitive under our experimental conditions. After one week contact time and subsequent ultracentrifugation, the supernatant was analyzed for dissolved Eu by γ-spectrometry. The m_{NaCl} values for Eu(III) (0.1, 0.9 and 3.9 m) slightly differ from those for Pu (0.1, 1.0 and 3.2 m). This has no impact on our conclusions. Previous work suggested no significant effect of incorporation reactions or sorption by secondary phases on Eu/Pu uptake between 1 week and 1 year [23].

2.4. Thermodynamic modeling

pH-pe diagrams for Pu were constructed using PhreePlot [30], which contains an embedded version of the geochemical speciation program PHREEQC [31]. Thermodynamic constants for Pu and Eu aqueous speciation were taken from the NEA thermodynamic database [32]. Lanthanides and actinides exhibit similar chemical behavior for the same redox state and chemical analogues are often used to estimate the complex geochemical behavior of Pu [14,33]. Therefore, in case of gaps in the Pu database, data for analogues were chosen (i.e. Eu(III), Np(IV), Np(V) and U(VI) for the respective Pu redox states). The specific ion interaction theory (SIT [12]) was used to calculate activity coefficients of aqueous species and the activity of water. These calculations are required in order to correct thermodynamic constants (including for redox equilibria) for ionic strength effects. SIT is generally considered valid for ionic strengths up to 3–4 m. The Pitzer model [13], which is valid for a larger range of ionic strengths but more complex than SIT, can also be applied to calculate activity coefficients for aqueous ions in concentrated media (see e.g. [3]). SIT and Pitzer equations are implemented in PHREEQC but only SIT was used in this study. At 25 °C, activity coefficients for an aqueous species *i* (γ_i) with a charge z_i are calculated as follows:

$$\log \gamma_i = -z_i^2 \frac{0.509 \times \sqrt{I}}{1 + 1.5\sqrt{I}} + \sum_k \varepsilon(i,k) \times m_k \quad (4)$$

where m_k is the molality of the aqueous species *k* (mol kg^{-1}), and ε (i,k) is the specific ion interaction coefficient between species *i* and *k* (kg mol^{-1}). Auxiliary reactions and constants are from the SIT database provided with PHREEQC (sit.dat file). All parameters involved in Pu and Eu aqueous speciation calculations are listed in Tables S1 and S2 in the supporting information.

The 2 SPNE SC/CE model was used to simulate Pu and Eu sorption to illite. The cation exchange capacity (CEC) of the illite was set to 0.225 eq kg^{-1} [34]. Only the strong sites of the 2 SPNE SC/CE model are considered in the adsorption calculations with a site density of 2×10^{-3} mol kg^{-1} [34]. The weak sites play a negligible role in our experiments, since a maximum loading of only 5×10^{-6} mol kg^{-1} is investigated (i.e. for $[Pu]_{tot} = 10^{-8}$ M). Surface complexation constants for Eu(III) and Pu(IV) extrapolated to zero ionic strength are available from previous work [23,34]. These constants accurately predict Eu(III), Pu(III) and Pu(IV) uptake on the present illite in 0.1 m NaCl [23]. A summary of the parameters for the 2 SPNE SC/CE model is given in supporting information (Table S3).

3. Results and discussion

3.1. Plutonium sorption to illite in solutions of different ionic strength

Results of log R_d for the Pu-illite system ($8 \times 10^{-11} < [Pu]_{tot} < 10^{-8}$ M) plotted versus pH_m for 0.1, 1 and 3.2 m NaCl are shown in Fig. 1a, b and c, respectively. Data for 0.1 m NaCl are taken from our previous work [23]. Experimental Pu sorption data in $0.1 < m_{NaCl} < 3.2$ m are plotted together for comparison on Fig. 1d. Generally, Pu uptake on illite increases with pH_m and remains constant for $pH_m > 6$. For $pH_m < 6$, Pu sorption decreases with increasing m_{NaCl}, whereas it is not affected by m_{NaCl} for $pH_m > 6$. Pu uptake data at 0.1 m NaCl is explained by accounting for the presence of both Pu(III) and Pu(IV) for $pH_m < 6$, where Pu (III) uptake is weaker than that of Pu(IV), whereas Pu(IV) prevails for $pH_m > 6$ [23]. Experimental data for Eu(III) (taken as a chemical analogue for Pu(III)) sorption to illite (for $m_{NaCl} = 0.1$, 0.9 and 3.9 m) are included in Fig. 1. In agreement with a recent study on Eu(III) sorption to illite in saline solutions [3], log R_d(Eu(III)) decreases with increasing m_{NaCl} for $pH_m < 6$, and is not affected by m_{NaCl} for $pH_m > 6$. The ionic strength dependence of log R_d(Pu) and log R_d(Eu) at $pH_m < 6$ is consistent with the assumption of a cation exchange mechanism being at least partly responsible for the uptake of Pu(III). Note, however, that our Pu uptake data for $pH_m < 6$ scatter significantly, which might be due to slight variations in redox conditions in individual batch experiments, as discussed later.

Fig. 2 shows all sorption data measured for $pH_m > 6$, $8 \times 10^{-11} < [Pu]_{tot} < 10^{-8}$ M and $m_{NaCl} = 0.1$, 1 and 3.2 m as log R_d versus the logarithm of the final Pu concentration in solution after phase separation ($\log[Pu]_{aq}$). Fig. 2 suggests that Pu uptake is not significantly influenced by $[Pu]_{tot}$ or ionic strength within the range of concentrations investigated and for $pH_m > 6$. $[Pu]_{aq}$ in presence of illite is close to or below the solubility limit of Pu(IV) in equilibrium with $PuO_{2(am,hydr)}$ ($10^{-10.4\pm0.5}$ M [35]). But the more or less constant R_d values even at the highest investigated Pu concentrations suggest the absence of significant precipitation or surface precipitation of $PuO_{2(am,hydr)}$. On average for all m_{NaCl} investigated, log $R_d = 5.3 \pm 0.3$ (1σ) for $pH_m > 6$, which is in excellent agreement with previous work in $m_{NaCl} = 0.1$ m ($\log R_d = 5.2 \pm 0.2$) [23].

Fig. 3 shows pe values of all our experiments plotted versus pH_m combined with the predominance diagram for Pu in solution for $m_{NaCl} = 0.1$ m. The corresponding predominance fields in 1 and 3.2 m NaCl shift because the activity coefficients of aqueous species vary with the ionic strength. Note that formation of aqueous

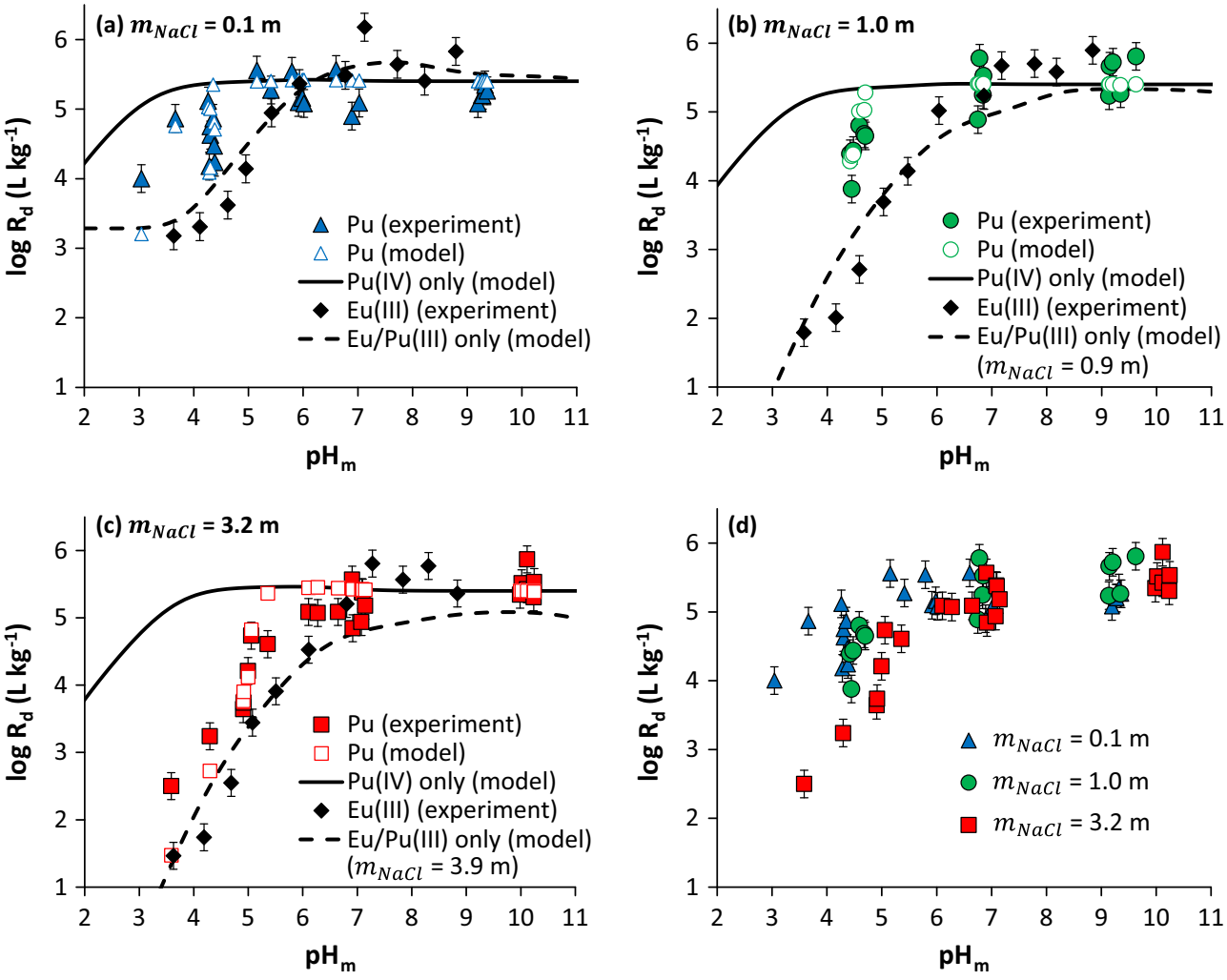

Fig. 1. Pu sorption to illite (log R_d in L kg^{-1}) versus pH_m (=$-\log m_{H^+}$) in (a) 0.1 (taken from our previous work [23]), (b) 1.0 and (c) 3.2 m NaCl. (d) Experimental Pu sorption data in 0.1 < m_{NaCl} < 3.2 m are plotted together for comparison. Experimental Eu(III)-illite sorption data for similar m_{NaCl} ((a) 0.1, (b) 0.9 and (c) 3.9 m NaCl) are shown for comparison. Solid and dashed lines show the predicted uptake of Pu(IV) (taken as independent component) and Eu/Pu(III), respectively. Empty symbols are model overall Pu sorption results using measured pH/pe values as input parameters.

Eu(III)- and Pu(IV)-Cl complexes is almost insignificant (<5%) for 0.1 < m_{NaCl} < 3.2 m (preliminary calculations not shown). However, the ionic strength dependence of the Pu(III)/Pu(IV) redox borderline is minor relative to the uncertainty of measured pe (see Fig. S1). In view of the scattered experimental pe data we are not able to clearly identify an ionic strength dependence of pH_m-pe values. The present results are in excellent agreement with previous studies in m_{NaCl} = 0.1 m [21,23]. The calculated predominance diagram and measured pH_m-pe values suggest that Pu(III) could predominate or exist in significant fractions at pH_m < 6 and Pu (IV) becomes dominant above this pH_m. The pronounced ionic strength dependence of Pu uptake (comparable to that of Eu) at low pH can thus easily be explained by the ion exchange competition between Pu^{3+} and Na^+ [3,23,34]. Based on our pH/pe data, we can also conclude that the ionic strength independent experimental Pu-illite sorption data at pH_m > 6 are due to the exclusive presence of Pu(IV) undergoing innersphere surface complexation only [6,31].

3.2. Modeling results

Pu(IV) uptake on illite is simulated for m_{NaCl} = 0.1, 1.0 and 3.2 m with the 2 SPNE SC/CE model. The same exercise is made for Eu(III) and m_{NaCl} = 0.1, 0.9 and 3.9 m. Previously reported surface complexation constants for Pu(IV) and Eu(III) are used for this purpose, without any parameter adjustment [23,34]. Results are shown in Fig. 1. In agreement with a previous study [3], the 2 SPNE SC/CE model accurately predicts the effect of high m_{NaCl} on Eu(III) uptake on the whole investigated pH_m range, when appropriate ionic strength corrections for the activity coefficients of aqueous species are applied with SIT. For pH_m < 6, Eu(III) sorption to illite decreases due to its competition with Na^+ for ion exchange sites whereas, for pH_m > 6, Eu(III) uptake is weakly affected by the ionic strength because of the formation of innersphere Eu-illite surface complexes [3]. Pu(IV) uptake on illite is predicted to be only weakly affected by the ionic strength in the range 0.1 < m_{NaCl} < 3.2 m. Model calculations agree with the observed absence of significant ionic strength effects on experimental uptake data of Th(IV) (taken as actinide analogue of Pu(IV)) on montmorillonite between 0.1 and 1.0 M $NaClO_4$ [4], and the sorption data for Pu obtained in the present study for pH_m > 6. These results support the assumption that tetravalent actinides undergo innersphere complexation rather than ion exchange at illite surface.

As previously inferred for actinide uptake on clays, the redox speciation of actinides is influenced by the formation of surface complexes [21–23]. The Pu(IV)/Pu(III) borderline at the illite

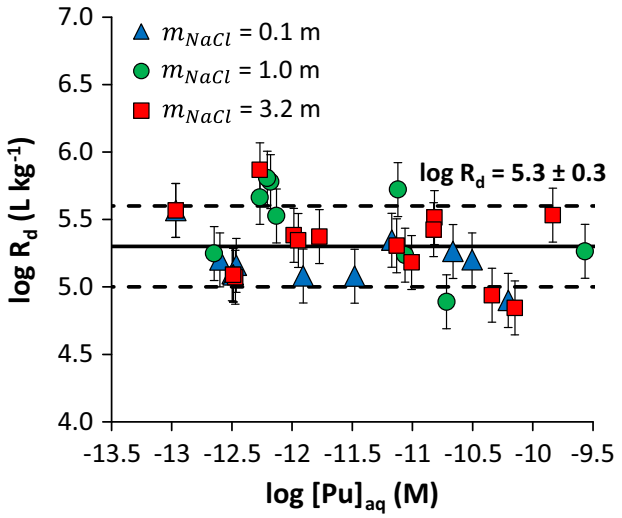

Fig. 2. Experimental data for Pu sorption onto illite (log R_d, in L kg^{-1}) versus the final Pu concentration in solution after phase separation (log $[Pu]_{aq}$, in M) for $pH_m > 6$ and $0.1 < m_{NaCl} < 3.2$ m (data for 0.1 m NaCl are taken from our previous work [23]). The average log R_d (=5.3) is shown as a line, associated with an uncertainty of ±0.3 (1σ; dashed lines).

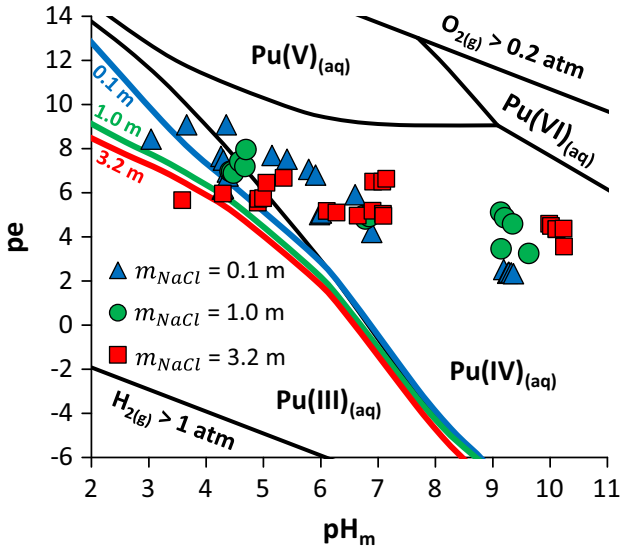

Fig. 3. The pe values measured in the illite suspensions in m_{NaCl} = 0.1, 1 and 3.2 m are plotted versus pH_m (=−log m_{H^+}). Data for 0.1 m NaCl are taken from our previous work [23]. The black lines correspond to the predominance pH_m-pe diagram for Pu in solution calculated for m_{NaCl} = 0.1 m and $[Pu]_{tot} = 10^{-11}$ M. The thick colored lines correspond to the Pu(IV)/Pu(III) borderline at the illite surface for m_{NaCl} = 0.1 m (blue), 1.0 m (green) and 3.2 m (red). (For interpretation of the references to color in this figure legend, the reader is referred to the web version of this article.)

surface (denoted as $\{Pu(IV)/Pu(III)\}_{surf}$) is expected to depend on the individual Pu(IV) and Pu(III) sorption behavior [22,23], and can be calculated for m_{NaCl} = 0.1, 1.0 and 3.2 m (Fig. 3) according to the following equation:

$$\{Pu(IV)/Pu(III)\}_{surf} = \{Pu(IV)/Pu(III)\}_{aq} + (\log R_d(Pu(III)) - \log R_d(Pu(IV))) \quad (5)$$

$\{Pu(IV)/Pu(III)\}_{aq}$ is the Pu(IV)/Pu(III) borderline in solution (i.e. plotted as a black line in Fig. 3), which is calculated using the Nernst equation. Values of log R_d(Pu(III)) and log R_d(Pu(IV)) in Eq. (5) represent the respective individual predicted uptake of the two Pu oxidation states under the same physico-chemical conditions (same pH, ionic strength, etc.), which can be seen in Fig. 1a–c ("Pu(IV) only" and "Pu(III) only"). For all investigated m_{NaCl} and $pH_m > 6$ log R_d(Pu(III)) ≈ log R_d(Pu(IV)) and, as a consequence, $\{Pu(IV)/Pu(III)\}_{aq}$ and $\{Pu(IV)/Pu(III)\}_{surf}$ coincide (Fig. 3). For pH < 6, $\{Pu(IV)/Pu(III)\}_{aq} > \{Pu(IV)/Pu(III)\}_{surf}$ because of the stronger sorption of Pu(IV) as compared to that of Pu(III). With increasing m_{NaCl}, log R_d(Pu(IV)) remains constant whereas log R_d(Pu(III)) decreases. Hence, $\{Pu(IV)/Pu(III)\}_{surf}$ decreases with increasing m_{NaCl} (i.e. the Pu(IV)/Pu(III) borderline at the illite surface is shifted to lower pe). According to this model, when the redox conditions (pH/pe) fall between $\{Pu(IV)/Pu(III)\}_{aq}$ and $\{Pu(IV)/Pu(III)\}_{surf}$, Pu(III) prevails in solution whereas Pu(IV) prevails at the illite surface, and the overall Pu uptake by illite is intermediate to the individual uptake of Pu in the two distinct oxidation states [22,23].

When different Pu redox states coexist, the overall uptake of actinides on clays highly depends on pe [21–23]. As pointed out before, R_d data scatter at acidic pH_m, which might be due to slight variations in redox conditions in individual batch experiments. The latter finding can be explained by the fact that the concentration of redox active components in the system is obviously low as discussed in a previous study on the interaction of Np with the same illite [21]. The exact nature of the redox partners determining measured pe values is not quite clear, but is most likely related to structurally bound Fe(II)/Fe(III). By using measured pH_m and pe values as model input parameters, overall Pu uptake onto illite is calculated using the 2 SPNE SC/CE model and SIT without further parameter adjustment. Model results are plotted as empty symbols on Fig. 1a–c. In addition, Fig. 4 shows predicted versus experimental log R_d values. Both figures show the good agreement between predicted and experimental Pu uptake onto illite. The average deviation between predicted and experimental results equals 0.3 log R_d units (shown as bold dashed lines), which corresponds to the experimental uncertainty. Larger deviation (maximum 1 log R_d units, shown as thin dashed lines) can be observed for some data, especially for the lowest log R_d values, which might be attributed to uncertainties in pe measurements (±0.8). Indeed, these data

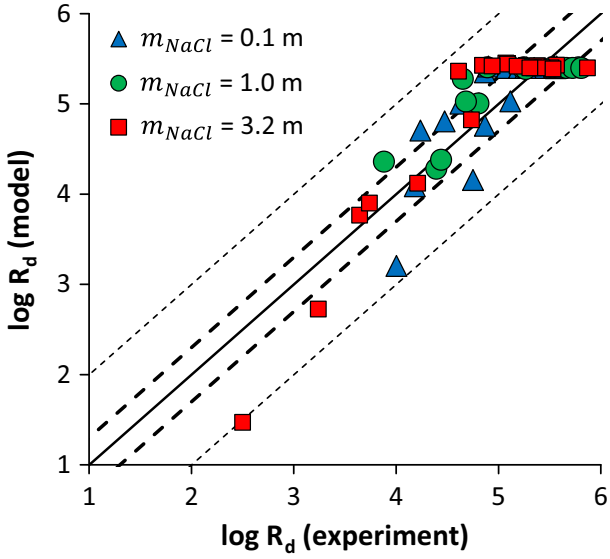

Fig. 4. Modeled versus experimental log R_d values for the whole dataset (present data for m_{NaCl} = 1.0 and 3.2 m and from our previous work for m_{NaCl} = 0.1 m [23]). The 1:1 (solid) line, associated with an uncertainty of ±0.3 log R_d units (bold dashed lines), which corresponds to both the experimental uncertainty on log R_d and the average deviation between experimental and modeled results, and an uncertainty of ±1 log R_d units (thin dashed lines), which corresponds to the largest deviation between experimental and modeled results.

were obtained in redox conditions (pH/pe) between {Pu(IV)/Pu(III)}$_{aq}$ and {Pu(IV)/Pu(III)}$_{surf}$ ($3 < pH_m < 6$; Fig. 3), for which predicted log R_d values highly depend on pe [21–23]. Therefore, it is possible to conclude that the present model can accurately predict Pu sorption to illite under a large range of pH_m, pe and ionic strength conditions.

4. Conclusions

In this study, we provided experimental data for Pu sorption to illite under slightly reducing conditions ($2 < pe < 10$), where the Pu(IV)/Pu(III) couple is involved, under saline conditions (up to 3.2 m NaCl), which are relevant for several potential deep geological nuclear waste repository sites. We observed that Pu sorption to illite was ionic strength dependent for $pH_m < 6$ because of the presence of Pu(III) and its competition with Na^+ for ion exchange sites. By contrast, Pu sorption to illite did not depend on the ionic strength for $pH_m > 6$, due to the predominance of Pu(IV), which undergoes innersphere surface complexation. According to our calculations, although Pu redox speciation in solution is only slightly influenced by NaCl concentration, Pu(IV)/Pu(III) redox equilibria at the illite surface can significantly be affected by the ionic strength when $pH_m < 6$. Overall Pu uptake could be accurately predicted by the 2 SPNE SC/CE model coupled to SIT. Results of the present work together with the outcome of previous investigations [3,21–23] demonstrate that the proposed modeling approach is robust and applicable, at least for the investigated systems, and might be a reliable predictive tool for performance assessment concerning clays under highly saline conditions. This recently developed approach now covers effects of pH, redox reactions and high background electrolyte concentrations, and allows estimating actinide sorption to clays at various redox conditions. Even at relatively low concentrations of redox governing components, measured pe still appears to be a meaningful parameter, which can be used to estimate retention of redox sensitive actinide ions as well as their redox speciation in solution and at the mineral surface with a quasi-mechanistic sorption model.

Nevertheless, the applicability of the approach to natural systems characterized by a high degree of heterogeneity and complexity still has to be demonstrated. Further studies dedicated to the uptake of actinides on natural soil- or clay rock formation-*in situ* porewater systems will be required to validate the present modeling approach. Our approach might also be tested for redox sensitive elements other than actinides (e.g. cerium, selenium, arsenic, chromium, iron) and adsorbing phases other than clays (e.g. oxides, natural organic matter).

Finally, non-electrostatic models were recently shown to be particularly suitable for the prediction of metal ion sorption to various types of surfaces in brines [3,9–11], which is further demonstrated in this study, and would find applications not only in the field of nuclear waste disposal but also, for instance, in marine chemistry.

Acknowledgements

This work was financed by the Federal Ministry of Economic Affairs and Energy (Germany) under contracts No. 02E10206 and 02E10961. The research leading to these results has received funding from the European Union's European Atomic Energy Community's (Euratom) Seventh Framework Program FP7/2007-2011 under grant agreement no. 249624 (CATCLAY project).

Appendix A. Supplementary material

Supplementary data associated with this article can be found, in the online version, at http://dx.doi.org/10.1016/j.jcis.2016.09.013.

References

[1] P. Vilks, Atomic Energy of Canada Limited, Toronto, Ontario, Canada, NWMO TR-2011-12, 2011.
[2] S. Nagasaki, T. Saito, T.T. Yang, J. Radioanal. Nucl. Chem. 308 (2016) 143.
[3] A. Schnurr, R. Marsac, T. Kupcik, T. Rabung, J. Lützenkirchen, H. Geckeis, Geochim. Cosmochim. Acta 151 (2015) 192.
[4] M.H. Bradbury, B. Baeyens, Geochim. Cosmochim. Acta 69 (2005) 875.
[5] M.H. Bradbury, B. Baeyens, Geochim. Cosmochim. Acta 73 (2009) 990.
[6] M.H. Bradbury, B. Baeyens, Geochim. Cosmochim. Acta 73 (2009) 1004.
[7] W. Brewitz, Zusammenfassender Zwischenbericht, GSF T 114, 1980.
[8] P. Fritz, S.K. Frape, Chem. Geol. 36 (1982) 179.
[9] J. Schijf, A.M. Ebling, Environ. Sci. Technol. 44 (2010) 1644.
[10] A. Zoll, J.A.M. Schjif, Geochim. Cosmochim. Acta 97 (2012) 183.
[11] D.A. Ams, J.S. Swanson, J.E.S. Szymanowski, J.B. Fein, M. Richmann, D.T. Reed, Geochim. Cosmochim. Acta 110 (2013) 45.
[12] L. Ciavatta, Anal. Chim. 70 (11-1) (1980) 551.
[13] K.S. Pitzer, CRC Press, Boca Raton, 1991.
[14] M. Altmaier, X. Gaona, T. Fanghanel, Chem. Rev. 113 (2013) 901.
[15] H. Geckeis, J. Lutzenkirchen, R. Polly, T. Rabung, M. Schmidt, Chem. Rev. 113 (2013) 1016.
[16] C.M. Marquardt, A. Seibert, R. Artinger, M.A. Denecke, B. Kuczewski, D. Schild, T. Fanghanel, Radiochim. Acta 92 (2004) 617.
[17] D.I. Kaplan, B.A. Powell, M.C. Duff, D.I. Demirkanli, M. Denham, R.A. Fjeld, F.J. Molz, Environ. Sci. Technol. 41 (2007) 7417.
[18] R.A. Buda, N.L. Banik, J.V. Kratz, N. Trautmann, Radiochim. Acta 96 (2008) 657.
[19] G. Lujanienė, J. Šapolaitė, E. Radžiutė, V. Aninkevičius, J. Radioanal. Nucl. Chem. 282 (2009) 793.
[20] R. Kirsch, D. Fellhauer, M. Altmaier, V. Neck, A. Rossberg, T. Fanghanel, L. Charlet, A.C. Scheinost, Environ. Sci. Technol. 45 (2011) 7267.
[21] R. Marsac, N.L. Banik, J. Lutzenkirchen, C.M. Marquardt, K. Dardenne, D. Schild, J. Rothe, A. Diascorn, T. Kupcik, T. Schafer, H. Geckeis, Geochim. Cosmochim. Acta 152 (2015) 39.
[22] R. Marsac, N.L. Banik, J. Lützenkirchen, R.A. Buda, J.V. Kratz, C.M. Marquardt, Chem. Geol. 400 (2015) 1.
[23] N.L. Banik, R. Marsac, J. Lützenkirchen, A. Diascorn, K. Bender, C.M. Marquardt, H. Geckeis, Environ. Sci. Technol. 50 (2016) 2092.
[24] M. Altmaier, V. Metz, V. Neck, R. Müller, Th. Fanghänel, Geochim. Cosmochim. Acta 67 (2003) 3595.
[25] M. Altmaier, X. Gaona, D. Fellhauer, G. Buckau, Intercomparison of redox determination methods on designed and near-neutral aqueous systems, Karlsruhe, 2010.
[26] B.A. Powell, R.A. Fjeld, D.I. Kaplan, J.T. Coates, S.M. Serkiz, Environ. Sci. Technol. 39 (7) (2005) 2107.
[27] M. Zavarin, B.A. Powell, M. Bourbin, P.H. Zhao, A.B. Kersting, Environ. Sci. Technol. 46 (5) (2012) 2692.
[28] J.D. Begg, M. Zavarin, P.H. Zhao, S.J. Tumey, B. Powell, A.B. Kersting, Environ. Sci. Technol. 47 (2013) 5146.
[29] A.E. Hixon, B.A. Powell, Environ. Sci. Technol. 48 (2014) 9255.
[30] D.G. Kinniburgh, D.M. Cooper, PhreePlot: Creating graphical output with PHREEQC <http://www.phreeplot.org>2009.
[31] D.L. Parkhurst, C.A. J. Appelo, User's guide to PHREEQC (Version 2) – a computer program for speciation, batch reaction, one-dimensional transport and inverse geochemical calculation; Denver, Colorado, 1999, pp. 312.
[32] R. Guillaumont, Th. Fanghänel, J. Fuger, I. Grenthe, V. Neck, D.A. Palmer, M.H. Rand, Update on the Chemical Thermodynamics of Uranium, Neptunium, Plutonium, Americium and Technetium, Elsevier, Amsterdam, 2003.
[33] G.R. Choppin, Radiochim. Acta 85 (1999) 89–95.
[34] M.H. Bradbury, B. Baeyens, H. Geckeis, T. Rabung, Geochim. Cosmochim. Acta 69 (2005) 5403.
[35] V. Neck, M. Altmaier, T. Fanghanel, C. R. Chim. 10 (2007) 959.